Electron paramagnetic resonance studies of Co^{2+} ions in congruent and nearly stoichiometric $LiNbO_3$ single crystals

1999 J. Phys.: Condens. Matter 11 4723

(http://iopscience.iop.org/0953-8984/11/24/313)

J. Phys.: Condens. Matter **11** (1999) 4723–4730. Printed in the UK PII: S0953-8984(99)99658-3

Electron paramagnetic resonance studies of Co^{2+} ions in congruent and nearly stoichiometric $LiNbO_3$ single crystals

Y N Choi†, I-W Park‡, S S Kim§, S S Park† and S H Choh†

† Department of Physics, Korea University, Seoul 136-701, Korea
‡ Seoul Branch, Korea Basic Science Institute, Seoul 136-701, Korea
§ Department of Physics, Changwon National University, Changwon 641-773, Korea

Received 25 November 1998, in final form 16 March 1999

Abstract. Congruent and nearly stoichiometric $LiNbO_3$ single crystals doped with Co^{2+} ions have been investigated by the electron paramagnetic resonance technique. The spin-Hamiltonian parameters, $g_\parallel = 2.671(2)$, $g_\perp = 5.052(2)$, $A_\parallel = 40(2) \times 10^{-4}$ cm^{-1}, and $A_\perp = 154(1) \times 10^{-4}$ cm^{-1}, are obtained without including the nuclear Zeeman and quadrupole interactions. The factor, k, of reduction due to the covalency is estimated as $0.92 \leqslant k \leqslant 1$ using the above g-values. On the basis of the temperature dependence of the linewidth, the spin–lattice relaxation and the spin–spin relaxation mechanisms are investigated. The former is a sum of a weak direct process with a phonon bottleneck ($\sim T^{2.4}$) and an Orbach process with $\Delta \sim 156$ cm^{-1} (or 225 K), and the latter is a sum of a typical temperature-independent process and an anomalous process with a temperature dependence $\propto T^{-3.6}$. This anomaly is considered as a shortening of T_2 due to the increase of the correlation length of the spin–spin interaction as the temperature decreases. The integrated signal intensity also showing an anomaly is a consequence of the linewidth anomaly.

1. Introduction

$LiNbO_3$ (LN) crystal is famous for its useful physical and chemical properties—e.g. ferroelectric, piezoelectric, electro-optical, and non-linear optical. Since it is not naturally available, it is usually grown by the Czochralski method. However, in general, there is slight mismatch of the composition ratio of [Li]/[Nb] even though the starting composition is exact. Consequently, there are intrinsic defects in crystals due to the Li deficiency. Among LN crystals, those having [Li]/[Nb] = 0.942 have been called congruent LN (CLN) [1], while those having [Li]/[Nb] = 1 are called stoichiometric. Various efforts to obtain stoichiometric LN, such as addition of a small amount of K_2O [2, 3], starting with a Li-rich composition [4–6], and vapour-transport-equilibrium (VTE) treatment [7–9], have been attempted.

Electron paramagnetic resonance (EPR) studies of Co^{2+} ions in LN crystals have been reported only for low temperature, since the linewidth increases exponentially with temperature due to the Orbach process [10, 11]. The local environment around the cations, Li and Nb, is a trigonally distorted octahedron of oxygen ions, and thus axial EPR spectra are expected.

In this work we report more refined spin-Hamiltonian parameters of Co^{2+} centres in a VTE-treated crystal and discuss the relaxation processes on the basis of the temperature dependence of the linewidth.

0953-8984/99/244723+08$19.50

2. Experimental procedure

2.1. Sample preparation

Single crystals of congruent lithium niobate, grown from melts of Li_2CO_3 (48.52 mol%) and Nb_2O_5 (51.48 mol%) powders using the Czochralski method at AKADEMIPEX in Hungary, were employed. Their composition ratio is not only non-stoichiometric but also the same as that of the melts. 0.02 mol% of Co^{2+} ions were added as an impurity. A thin slab (thickness $\sim$1 mm) of the congruent $LiNbO_3$ crystal, [Li]/[Nb] = 0.942, was treated by the VTE process to obtain a nearly stoichiometric crystal [1]. A schematic diagram of the VTE process is given as figure 1. During the VTE process, Li ions from the two-phase powder were diffused into the thin slab of CLN crystal so that the Li deficiency in the CLN crystal was reduced. Among the various techniques tried in efforts to obtain stoichiometric LN crystals, the VTE treatment was found to be one of the most efficient, since the Li deficiency of a non-stoichiometric crystal was made up for during the process [1].

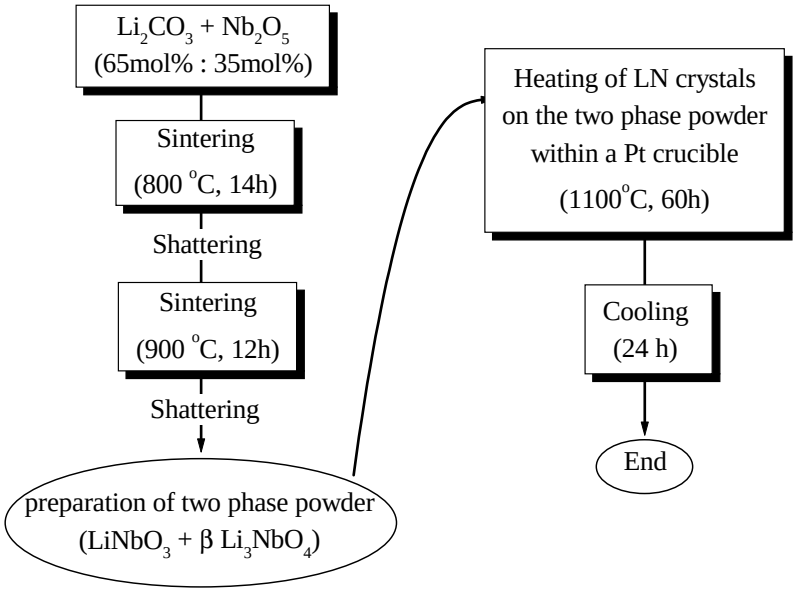

Figure 1. A block diagram of the VTE process. A thin LN crystal was laid on the curled platinum wire embedded in the Li-rich two-phase powder and heated at 1100 °C for 60 hours.

2.2. EPR measurements

EPR measurements of $Co^{2+}(3d^7)$ ions in a CLN crystal and a nearly stoichiometric $LiNbO_3$ crystal (VLN: VTE-treated LN) were carried out by employing a Bruker ESP300 X-band spectrometer. A rapid decrease of the relaxation time with increasing temperature (Orbach relaxation) prevented us from making measurements above $\sim$30 K. Since the EPR spectra of Co^{2+} in CLN and VLN crystals both show axial symmetry ($C_3 \parallel \boldsymbol{c}$), the rotation pattern of the spectra has been recorded only in the ca-plane. In order to examine the relaxation mechanism, the temperature dependences of the Co^{2+} EPR spectra were recorded with the magnetic field parallel to the a-axis.

3. Experimental results and discussion

3.1. The rotation pattern and spin Hamiltonian

The orbital ground state of the free Co^{2+} ion is ^4F and its electronic configuration is $[Ar]3d^7$. It has three unpaired electrons in the d shell, so its total electron spin S is 3/2.

For the Co^{2+} ion in an octahedral crystal field, the orbital ground state of the ground term ^4F is the T_{1g} triplet. Assuming a moderate spin–orbit interaction, one can easily calculate the isotropic g-value as 4.33 from crystal-field theory without mixing the excited triplet state, $|^4P, T_{1g}\rangle$, and covalency effect. The observed average g-value, $(g_\parallel + 2g_\perp)/3 = 4.258$, is similar to the isotropic one, but there is a significant anisotropy. This anisotropy can be explained in terms of the ground state of the trigonally distorted octahedral crystal field, as follows [12]:

$$|\tilde{J}' = 1/2, \tilde{J}'_z = \pm 1/2\rangle = \frac{1}{\sqrt{N}}(|J' = 1/2, J'_z = \pm 1/2\rangle + a|3/2, \pm 1/2\rangle + b|5/2, \pm 1/2\rangle) \tag{1}$$

where $\boldsymbol{J}' = \boldsymbol{L}' + \boldsymbol{S}$ is the direct sum of the effective orbital and the electron spin angular momenta under octahedral symmetry ($J' = 1/2$, 3/2 or 5/2), $\tilde{\boldsymbol{J}}'$ is the total angular momentum perturbed by a small trigonal distortion, and $\sqrt{N} = \sqrt{1 + a^2 + b^2}$ is a normalization constant which could be approximated as 1 since $b^2 \ll a^2 \ll 1$. Then the g-values for the spin–orbit interaction can be calculated from the energy eigenvalues of the electronic Zeeman interaction, $H_{eZ} = \beta \boldsymbol{B} \cdot (g_l \boldsymbol{L}' + g_s \boldsymbol{S})$, as follows:

$$g_\parallel = \tfrac{1}{3}(5g_s - 2g_l) + \tfrac{4}{3}\sqrt{5}(g_s - g_l)a + \tfrac{1}{15}(11g_s + 4g_l)a^2 + \tfrac{1}{5}(3g_s + 2g_l)b^2 + \tfrac{4}{5}(g_s - g_l)ab$$
$$\approx \tfrac{1}{3}(5g_s - 2g_l) + \tfrac{4}{3}\sqrt{5}(g_s - g_l)a \tag{2}$$

$$g_\perp = \tfrac{1}{3}(5g_s - 2g_l) - \tfrac{2}{3}\sqrt{5}(g_s - g_l)a - \tfrac{2}{15}(11g_s + 4g_l)a^2 + \tfrac{3}{5}(3g_s + 2g_l)b^2 + \tfrac{6}{5}(g_s - g_l)ab$$
$$\approx \tfrac{1}{3}(5g_s - 2g_l) - \tfrac{2}{3}\sqrt{5}(g_s - g_l)a \tag{3}$$

where $g_s = 2.0023$ is the g-value of the free electron, $g_l = -\alpha k = -\frac{1}{2}(3 - 5\tau^2)k$ is an effective orbital g-value, τ^2 is the probability that the system is in the excited state (^4P), and k is a reduction factor due to the covalency. The above equations have been rederived, since we found minor errors in the corresponding equations (7.105) in reference [12]. By substituting in experimental g-values from table 1, $g_\parallel = 2.671$ and $g_\perp = 5.052$, one obtains $a = -0.158$ and $g_l = -1.40$. From the above calculation it can be stated that the probability of the system being in the $|3/2, \pm 1/2\rangle$ state is about $a^2 = 2.50\%$ and the reduction factor for the covalency lies between 0.92 (for $\tau = 0$) and 1.0 (for $\tau = 0.22$ or $\tau^2 = 4.8\%$). The last result means that the chemical bonding between the Co^{2+} ion and the oxygen ion is much more ionic than the previous finding ($k = 0.7$) [11]. The energy splitting between the ground ($|\tilde{J}' = 1/2\rangle$) and first excited state ($|\tilde{J}' = 3/2\rangle$) in an octahedral field, $\Delta = \frac{3}{2}|\lambda_{eff}| = \frac{3}{2}|g_l\lambda| \sim 370\ cm^{-1}$, is larger than the reported value, 100 cm^{-1} [11], and the measured one, $156 \pm 7\ cm^{-1}$. Therefore, further interactions must be included to reduce Δ to 156 cm^{-1}. The spin–orbit interaction may

Table 1. Spin-Hamiltonian parameters of the Co^{2+} centre in $LiNbO_3$.

$g_\parallel$	$g_\perp$	$A_\parallel$ (10^{-4} cm^{-1})	$A_\perp$ (10^{-4} cm^{-1})	References
2.62	4.98(1)*	$\leqslant 49$	157	[10]
2.59	5.04	~ 0	153	[11]
2.671(2)	5.052(2)	40(2)	154(1)	Present work ($T = 4.3$ K)

* Numbers in parentheses are the uncertainties of the final digits.

be perturbed by a weak Jahn–Teller coupling ($H_{JT} \ll H_{so}$) which does not change the average g-value from the isotropic one and causes a decrease of the energy splitting [11]. A possible energy diagram of the system is shown in figure 2.

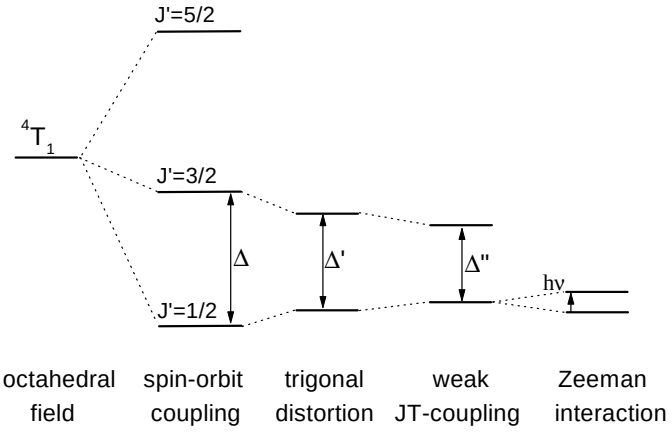

Figure 2. A possible energy level diagram of Co^{2+} ions in a LN crystal. The higher states under the octahedral crystal field are omitted. The trigonal distortion reduces the splitting due to the spin–orbit coupling, and the weak Jahn–Teller coupling also reduces it further ($\Delta'' < \Delta' < \Delta$). The allowed EPR transition due to the Zeeman interaction is shown by the arrow.

The energy separation between the ground state and the first excited state is very large compared with the thermal energy. Hence it is common to introduce an effective spin of $S' = 1/2$ (hereafter the prime will be omitted) for describing the EPR of Co^{2+} ions; the zero-field splitting term is not needed. The ^{59}Co nucleus, of 100% natural abundance, has a nuclear spin of $I = 7/2$, and hence hyperfine, nuclear Zeeman, and nuclear quadrupole interactions are expected. However, the last two interactions are in general very weak compared with the major interactions at the X-band, so the following effective spin Hamiltonian is adopted in this study:

$$H = \beta \boldsymbol{B} \cdot \tilde{\mathbf{g}} \cdot \boldsymbol{S} + \boldsymbol{I} \cdot \tilde{\mathbf{A}} \cdot \boldsymbol{S}. \tag{4}$$

The spin-Hamiltonian parameters of Co^{2+} ions in CLN and VLN turn out to be identical within experimental uncertainties. As shown in table 1, we could determine more accurate values, particularly of $g_{\parallel}$ and $A_{\parallel}$, than previous workers [10, 11]. The linewidths of the Co^{2+} ion in CLN are much broader than those for VLN, as displayed in figure 3. As a consequence, the hyperfine structure is not resolved near the c-axis for CLN, while it is resolved for VLN. This can be explained by the concentration of Li vacancies, since CLN has many more Li vacancies than VLN. As a result, the local environment around the Co^{2+} ion may have a Li vacancy nearby, which may cause an inhomogeneous broadening of the linewidth for CLN.

There are some extra signals in addition to the main hyperfine lines for CLN as indicated by the small vertical arrows in figure 3(a), but these are hardly noticeable for VLN (figure 3(b)). These extra signals were postulated as originating from either the Co^{4+} ion at the same site [10] or Co^{2+} at a lower-symmetry site [11]. Since Co^{4+} is an S-state ion, its g-value should be close to 2, which is very different from the experimental result. Therefore, with the former postulate of Co^{4+}, it cannot explain the reduction of the extra signals for the VLN crystal. Since CLN is less stoichiometric than VLN, there are more Li deficiencies in CLN, and hence it may have different environments around the Co^{2+} ion. However, in VLN, all of the local environments of Co^{2+} ions are nearly equivalent; thus only one set of hyperfine signals results. So we confirm that the origin of the extra signals is related to Li vacancies near the Co^{2+} ion, i.e. the lower-symmetry Co^{2+} sites are responsible for the additional signals.

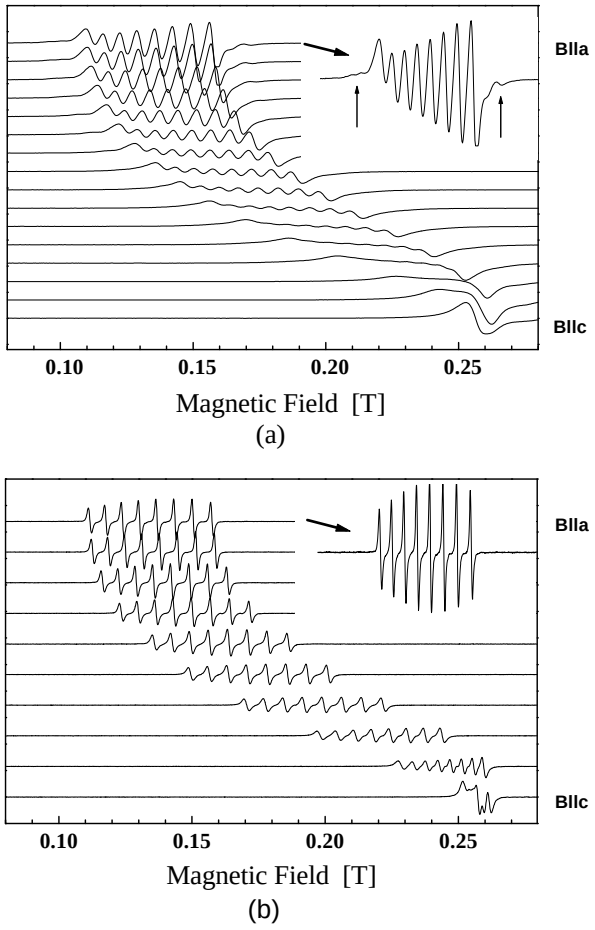

Figure 3. The rotation pattern of the Co^{2+} EPR spectra measured with an X-band frequency (9.250 GHz) for (a) CLN and (b) VLN crystals at $T = 4.3$ K. The signals in (a) marked with vertical arrows may be resulting from Li deficiencies. The intervals of the rotation angles are 6° for (a) and 10° for (b).

3.2. Hyperfine spacing

The spacings of the Co^{2+} hyperfine lines measured with the microwave power 1 μW were recorded at $T = 4.8$ K with the magnetic field parallel to the a-axis. As shown in figure 4, the line spacing increases linearly with the nuclear magnetic quantum number, m. This can be explained by means of the calculation of the second-order perturbation of the hyperfine interaction with respect to the electronic Zeeman term in axial symmetry [13]:

$$H = \beta[g_\parallel S_z B_z + g_\perp (S_x B_x + S_y B_y)] + A_\parallel S_z I_z + A_\perp (S_x I_x + S_y I_y). \tag{5}$$

The resonance condition of the energy eigenvalues, when the magnetic field is parallel to the a-axis, is given by

$$h\nu = E(1/2, m) - E(-1/2, m) = g_\perp \beta B + A_\perp m + \frac{A_\parallel^2 + A_\perp^2}{4 g_\perp \beta B_0}\left(\frac{63}{4} - m^2\right) \tag{6}$$

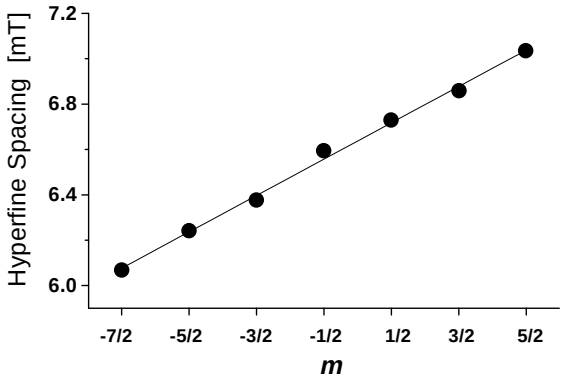

Figure 4. The hyperfine-line spacing of Co^{2+} in a VLN crystal with the magnetic field parallel to the a-axis at $T = 4.8$ K. A weak microwave power (1 μW) was applied in order to avoid saturation. Dots are experimental data and the line is a linear fit to them.

where $B_0 = h\nu/g_\perp\beta$. From equation (6), the hyperfine line spacing is obtained as

$$\Delta B_{hf} \approx \frac{A_\perp}{g_\perp\beta}\left[1 + \frac{A_\parallel^2 + A_\perp^2}{4(h\nu)A_\perp} - \frac{15}{16}\frac{A_\parallel^2 + A_\perp^2}{(h\nu)^2}\right] - \frac{A_\parallel^2 + A_\perp^2}{2(h\nu)g_\perp\beta}\left[1 - \frac{6A_\perp}{h\nu}\right]m \tag{7}$$

which shows a linear dependence on m. On substituting the spin-Hamiltonian parameters obtained into equation (7), the straight line in figure 4 is obtained. In this calculation, although the nuclear Zeeman and quadrupole terms of ^{59}Co are neglected, the calculated result is in good agreement with the experimental data since the nuclear Zeeman interaction is about 2000 times smaller than the electronic Zeeman interaction and the nuclear quadrupole interaction is comparable to the nuclear Zeeman interaction.

3.3. The temperature dependences of the linewidth and the integrated signal intensity

By measuring the temperature dependence of the linewidth of the Co^{2+} signals, the relaxation times and their mechanisms have been investigated. The linewidth is measured as the peak-to-peak width of the first-derivative signal and the intensity is obtained from the double integration of the first-derivative signal. As displayed in figure 5, distinct temperature dependences of the linewidth and of the intensity are observed. The relation between the linewidth ΔB and the relaxation times is generally given by the following equation:

$$(g\beta/\hbar)\Delta B = 1/T_2^* = 1/T_2 + 1/(2T_1) \tag{8}$$

where T_2^* is the effective transverse relaxation time. The fitting formula for the experimental data is obtained as

$$\Delta B\ (\mathrm{mT}) = [A + B/T^r] + [CT^s + D\exp(-\Delta/T)] \tag{9}$$

where $A = 0.93(\pm0.02)$, $B = 3.8(\pm2) \times 10^2$, $C = 8.3(\pm4) \times 10^{-10}$, $D = 6.8(\pm2) \times 10^3$, $r = 3.6(\pm0.4)$, $s = 2.4(\pm0.3)$, and $\Delta = 225(\pm10)$ K, equivalent to $156(\pm7)$ cm^{-1}, and the temperature is in units of K. To obtain the above parameters, the data for the lowest temperature in figure 5 were excluded. Terms in the first square bracket are contributions from the spin–spin relaxation. The constant term represents a temperature-independent typical spin–spin relaxation, and the other term is postulated from the following argument. As T decreases, the correlation length of the spin–spin interaction increases up to the mean distance l of the nearest Co^{2+} ions (one ion per $\simeq$17 units of LN), since the correlation length decreases due to the scattering by phonons. Below about 11 K, the correlation length might become comparable to or exceed l as the temperature decreases. Therefore, the correlation time of the spin–spin interaction decreases (or the linewidth increases) as T decreases, but it will cease to decrease

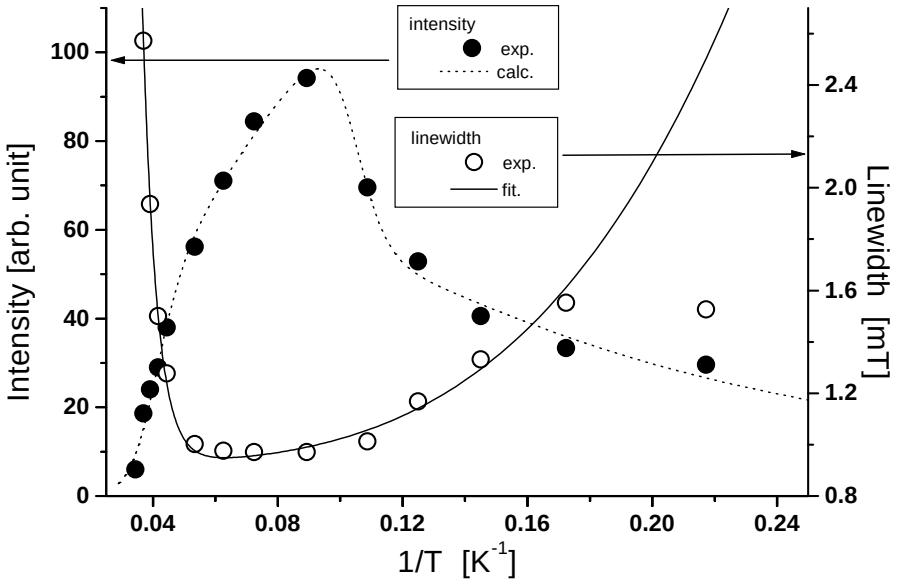

Figure 5. The linewidth and integrated intensity of the Co^{2+} ion in a VLN crystal as functions of the reciprocal temperature. Circles are experimental data and curves are fitted (solid) and calculated (dotted) results, obtained using the formulae (9) and (10) given in the text.

at temperatures lower than 11 K, as in figure 5, because the correlation length will already have covered the effective range of spin–spin interaction. This is why the data for the lowest temperature, 4.6 K, were excluded from the parameter fitting. The other two terms in the last square bracket represent a spin–lattice relaxation of a weak direct process with a phonon bottleneck ($\sim T^{2.4}$) and the well known Orbach process, respectively.

Generally, the intensity is expected to grow as the temperature decreases. However, an anomalous behaviour of the integrated intensity, diminishing as T decreases, appears below $\sim$11 K. The experimental data are fitted to the following formula, which is the power absorbed by the spin system:

$$\text{integrated intensity} = \frac{C_1(C_2/T)T_2^*}{1 + 2T_1T_2^*C_2} \tag{10}$$

where C_1 and C_2 are constants and T is the temperature [14]. By employing equation (10), the temperature dependence of the integrated intensity can be nicely fitted with the dotted curve shown in figure 5. Therefore the anomaly of the integrated intensity can be understood as a consequence of the linewidth, or the relaxation anomaly.

4. Summary

From rotation patterns of Co^{2+} EPR spectra for a VLN crystal, the spin-Hamiltonian parameters are determined more accurately than by previous workers who employed less stoichiometric LN crystals, since the linewidths are much narrower for VLN than for other crystals. The spin-Hamiltonian parameters are found to be identical for the two kinds of crystal, CLN and VLN, that we investigated. The lower bound of the reduction factor due to the covalency is calculated as 0.92 (8% reduction) from the experimental g-values, which means that the bonding between the Co^{2+} ion and the O^{2-} ion in LN crystal is much more ionic than in

other host crystals. In order to explain the energy splitting between the ground state and the first excited state of Co^{2+} in the $LiNbO_3$ host, obtained from the temperature variation of the linewidths, a weak trigonal crystal field ($\Delta_{so} \rightarrow \Delta'_{so}$) and a weak Jahn–Teller splitting ($\Delta'_{so} \rightarrow \Delta''_{so}$) are introduced. The hyperfine spacing measured at 4.8 K with $\boldsymbol{B} \parallel a$-axis is in good agreement with the calculation of the second-order perturbation of the hyperfine interaction with respect to the electronic Zeeman interaction without any nuclear interactions. The additional signals appearing for CLN may well be due to Li vacancies, because those signals are hardly noticeable for VLN, which has far fewer Li vacancies than CLN.

The temperature dependencies of the linewidth and intensity both show anomalies below $\sim$11 K. As the temperature decreases, the linewidth increases, and the intensity decreases, which is beyond the general expectation. From equations (8), (9), and (10), the spin–spin and spin–lattice relaxation processes are factored out. The spin–spin relaxation is composed of a temperature-independent typical spin–spin relaxation process and an anomalous process represented by the term in $T^{-3.6}$. A possible explanation for the process is that as the temperature decreases below $\sim$11 K, the correlation length of the spin–spin interaction may increase and become comparable to or exceed the mean distance of the nearest Co^{2+} ions, resulting in the correlation time being shortened. The anomalous temperature dependence of the integrated signal intensity, which shows a decrease of the intensity as the temperature decreases below $\sim$11 K, is a consequence of the linewidth anomaly, since it can be reproduced from equation (10). And the spin–lattice relaxation is a sum of the direct process with a phonon bottleneck, $\sim T^{2.4}$, and a well known Orbach process.

Acknowledgments

This work was supported by the KOSEF through the RCDAMP at Pusan National University (1997–2000), and one of authors (YNC) is grateful for a pre-doctoral scholarship (1998) from the Korea Research Foundation.

References

[1] Abrahams S C and Marsh P 1971 *Acta Crystallogr.* B **42** 61
[2] Carruthers J R, Peterson G E, Grasso M and Bridenbaugh P M 1971 *J. Appl. Phys.* **42** 1846
[3] Furukawa Y, Sato M, Kitamura K, Yajima Y and Minakata M 1992 *J. Appl. Phys.* **72** 3250
[4] Malovichko G I, Grachev V A, Yurchenko L P, Proshko V Y, Kokanyan E P and Gabrielyan V T 1992 *Phys. Status Solidi* a **133** K29
[5] Malovichko G I, Grachev V A, Kokanyan E P, Betzler O F, Gather B, Jermann F, Klauer S, Schlarb U and Wöhlecke M 1993 *Appl. Phys.* A **56** 103
[6] Malovichko G I, Cerclier O, Estienne J, Grachev V A, Kokanyan E P and Boulesterix C 1995 *J. Phys. Chem. Solids* **56** 1285
[7] Bordui P E, Norwood R G, Jundt D H and Fejer M M 1992 *J. Appl. Phys.* **71** 875
[8] Gröne A and Kapphan S 1995 *J. Phys. Chem. Solids* **56** 687
[9] Choi Y N, Choh S H, Park I-W, Koh E K and Kim S S 1998 *J. Korean Phys. Soc.* **32** S643
[10] Mirzakhanyan A A and Petrosyan A K 1986 *Sov. Phys.–Solid State* **28** 904
[11] Donnerberg H J and Shirmer O F 1987 *Solid State Commun.* **63** 29
[12] Abragam A and Bleaney B 1986 *Electron Paramagnetic Resonance of Transition Ions* (New York: Dover) ch 7
[13] Abragam A and Bleaney B 1986 *Electron Paramagnetic Resonance of Transition Ions* (New York: Dover) ch 3
[14] Pilbrow J R 1990 *Transition Ion Electron Paramagnetic Resonance* (Oxford: Clarendon) ch 8